View metadata, citation and similar papers at core.ac.uk
brought to you by CORE
provided by Carolina Digital Repository

THE JOURNAL OF BIOLOGICAL CHEMISTRY
Vol. 275, No. 39, Issue of September 29, pp. 30378–30386, 2000
© 2000 by The American Society for Biochemistry and Molecular Biology, Inc.
Printed in U.S.A.

Characterization of the Histone H1-binding Protein, NASP, as a Cell Cycle-regulated Somatic Protein*

Received for publication, May 4, 2000, and in revised form, July 10, 2000
Published, JBC Papers in Press, July 12, 2000, DOI 10.1074/jbc.M003781200

Richard T. Richardson, Iglika N. Batova‡, Esther E. Widgren, Lian-Xing Zheng§, Michael Whitfield§, William F. Marzluff§, and Michael G. O'Rand¶

From the Department of Cell Biology and Anatomy and the §Program in Molecular Biology and Biotechnology, University of North Carolina at Chapel Hill, North Carolina 27599

Nuclear autoantigenic sperm protein (NASP), initially described as a highly autoimmunogenic testis and sperm-specific protein, is a histone-binding protein that is a homologue of the N1/N2 gene expressed in oocytes of *Xenopus laevis*. Here, we report a somatic form of NASP (sNASP) present in all mitotic cells examined, including mouse embryonic cells and several mouse and human tissue culture cell lines. Affinity chromatography and histone isolation demonstrate that NASP from myeloma cells is complexed only with H1, linker histones. Somatic NASP is a shorter version of testicular NASP (tNASP) with two deletions in the coding region arising from alternative splicing and differs from tNASP in its 5′ untranslated regions. We examined the relationship between NASP mRNA expression and the cell cycle and report that in cultures of synchronized mouse 3T3 cells and HeLa cells sNASP mRNA levels increase during S-phase and decline in G_2, concomitant with histone mRNA levels. NASP protein levels remain stable in these cells but become undetectable in confluent cultures of nondividing CV-1 cells and in nonmitotic cells in various body tissues. Expression of sNASP mRNA is regulated during the cell cycle and, consistent with a role as a histone transport protein, NASP mRNA expression parallels histone mRNA expression.

NASP,[1] initially described as a highly autoimmunogenic testis and sperm-specific protein, is present in the nucleus of spermatozoa and spermatogenic cells (1–3), hence the name nuclear autoantigenic sperm protein. Previous studies (4) have demonstrated that human NASP contains three functional histone binding sites: site I (amino acids 116–127), site II, (amino acids 469–512), and site III (amino acids 211–244). *In vitro*, recombinant NASP will bind both linker and core histones (4).[2] As a histone-binding protein (4, 5), NASP appears to be a homologue of the N1/N2 gene expressed in oocytes of *Xenopus laevis* (6–9) because, in addition to the conserved coding regions, there is an almost 60% identity between the 3′ untranslated regions of rabbit NASP and *Xenopus* N1/N2 mRNAs (2). In *Xenopus* oocytes, the non-chromatin-bound core histones H3 and H4 are associated in a complex with N1/N2 (10, 11), providing a mechanism for the storage of histones for DNA replication in the early embryo. Both mouse (12) and sea urchin oocytes (13) also store histones in a non-chromatin-bound form. Other mammalian histone-binding proteins, for example the nucleosome assembly factor NAP-1 (14–17), the chromatin assembly factor CAF-1 (18–21), and the transcription proteins HIRA-HIRIP3 (22), not only bind histones but appear to be important for the assembly of chromatin (19, 23–26). Consequently NASP may be important not only for both the storage and transport of histones but also for the assembly of chromatin.

Here, we report a somatic form of NASP (sNASP) present in almost all tissues examined, including mouse embryonic cells and several mouse and human tissue culture cell lines. Interestingly, an analysis of the histones complexed with NASP *in vivo* revealed that in mouse myeloma 66-2 cells only H1, linker histones, could be detected. Somatic NASP is a shorter version of the testicular form of NASP (tNASP) with two deletions in the coding region arising from alternative splicing and differing from tNASP in its 5′ untranslated regions. In both embryonic and transformed cell lines in culture, we found that both sNASP and tNASP are expressed. Unlike spermatogenesis in the testis, in which DNA replication and histone synthesis are uncoupled, in somatic cells histone synthesis and histone mRNA levels are closely coupled to DNA replication (27–29). Having found that NASP is present in somatic cells, we therefore also examined the relationship between NASP mRNA expression and the cell cycle and report that sNASP mRNA levels increase during S-phase and decline during G_2, concomitant with histone mRNA levels.

EXPERIMENTAL PROCEDURES

All reagents and chemicals used in this study were of molecular biology grade. Alkaline phosphatase, peroxidase, and fluorescein isothiocyanate-labeled goat anti-rabbit (heavy and light chain) antisera were purchased from Organon Technica, Inc. (West Chester, PA). DNA probes were labeled with either a North2South biotin-DNA labeling kit (Pierce) or [^{32}P-rsqb]dCTP (ICN Biomedicals Inc., Costa Mesa, CA) with Ready To Go DNA labeling beads (Amersham Pharmacia Biotech). All oligonucleotides were synthesized at the University of North Carolina-

* This research was supported by NICHD, National Institutes of Health, through Cooperative Agreement U54HD35041 as part of the Specialized Cooperative Centers Program in Reproductive Research. The costs of publication of this article were defrayed in part by the payment of page charges. This article must therefore be hereby marked "*advertisement*" in accordance with 18 U.S.C. Section 1734 solely to indicate this fact.

The nucleotide sequence(s) reported in this paper has been submitted to the GenBank™/EBI Data Bank with accession number(s) AF034610 (tNASP), AF095722 (sNASP).

‡ Present address: Dept. of Immunobiology, Bulgarian Academy of Sciences, Sofia 1113, Bulgaria.

¶ To whom correspondence should be addressed: Dept. of Cell Biology and Anatomy, CB #7090, University of North Carolina at Chapel Hill, Chapel Hill, NC 27599-7090. Tel.: 919-966-5698; Fax: 919-966-1856; E-mail: morand@unc.edu.

[1] The abbreviations used are: NASP, nuclear autoantigenic sperm protein; sNASP, somatic form of NASP; tNASP, testicular NASP; PCR, polymerase chain reaction; bp, base pair(s); kb, kilobase; PBS, phosphate-buffered saline; G3PDH, glyceraldehyde-3-phosphate dehydrogenase; FACS, fluorescence-activated cell sorter; HPLC, high pressure liquid chromatography; UTR, untranslated region.

[2] I. N. Batova and M. G. O'Rand, unpublished observations.

This paper is available on line at http://www.jbc.org

This is an Open Access article under the CC BY license.

Chapel Hill (UNC-CH) Nucleic Acids Core Facility. Restriction and modifying enzymes were purchased from New England Biolabs, Inc. (Beverly, MA). Purifications of plasmid DNA and PCR products were carried out using QIAprep Miniprep and QIAquick PCR purification kits, respectively (Qiagen Inc., Valencia, CA).

Library Screening and Sequencing

The mouse testis cDNA library was described previously (30), and the mouse ovary cDNA library was a gift from Dr. Jurrien Dean (National Institutes of Health, Bethesda, MD). Screening by colony hybridization was performed with ^{32}P-labeled probes using Express-Hyb Solution (CLONTECH, Inc., Palo Alto, CA) according to the recommended protocol. Both strands of positive clones were sequenced by the UNC-CH automated sequencing facility on a model 377 DNA sequencer using the ABI Prism rhodamine terminator cycle sequencing kit (Applied Biosystems Inc., Foster City, CA). The sequence for mouse tNASP (Fig. 1) was obtained by screening a mouse testis cDNA library with a rabbit tNASP probe (2). The sequence for sNASP (Fig. 1) was obtained by screening a mouse ovary cDNA library with mouse tNASP cDNA. Sequence manipulations and analyses were performed using DNAsis software (Hitachi Software Inc., San Francisco, CA).

Northern Blots

Northern blots (Fig. 2, a multiple tissue Northern blot; Fig. 3, an RNA master blot (CLONTECH)) were probed with ^{32}P-labeled full-length tNASP, generated by PCR primers specific to the coding region of tNASP (nt 92–2414), and hybridized using Express-Hyb Solution according to the CLONTECH protocol. Blots were exposed for 16 h on a phosphorImager screen, scanned using a Molecular Dynamics Storm 860 PhosphorImager (Amersham Pharmacia Biotech), and analyzed and quantitated using either ImageQuant software (ImageQuant, Inc., Sunnyvale, CA) or GelExpert software (Nucleotech, Inc., San Mateo, CA). Northern blots of HeLa cell and mouse 3T3 fibroblast RNA were prepared from 1.2% agarose gels loaded with 5 μg/well total RNA and electrophoresed as described for low percentage formaldehyde gels in the Qiagen RNeasy Mini Kit handbook. After electrophoresis, the gels were capillary-transferred to Hybond-N (Amersham Pharmacia Biotech).

PCR Analysis

Gene expression in a variety of tissues was studied using the multiple tissue cDNA panel (CLONTECH). CLONTECH cDNAs are normalized to eight different housekeeping genes. cDNAs from thymus and ovary were prepared in our laboratory, but these were not normalized to different housekeeping genes. Thymus and ovary cDNAs were prepared as follows. RNA was isolated from the tissue according to the manufacturer's instructions using the RNeasy Mini Kit for Total RNA (Qiagen) and cDNA was prepared from an oligo(dT) primer using a SuperScript preamplication system for first-strand cDNA synthesis (Life Technologies, Inc.). PCRs were performed using Ready To Go PCR beads (Amersham Pharmacia Biotech). Cycle conditions were set up as described previously (23) using the following primers: for amplification of the full-length NASP coding region, the sense primer was 5′-ATGGCCACAGATTCTACAGCC-3′ and the antisense primer was 5′-TTAACATGCAGTGCTTTT-3′; for amplification of a fragment specific for tNASP, the sense primer was 5′-AATGAGTGTGGGGAAGCC-3′ and the antisense primer was 5′-TTCACTCTCAGAGGTAGC-3′.

Antisera

Rabbits were immunized with purified recombinant proteins as described (31). Expression constructs were produced using PCR, cloned into pQE-30, transformed to bacterial host M15 (pREP-4) for expression, and purified on Ni-NTA resin as described (31). N-terminal (nucleotides 96–1099) and C-terminal (nucleotides 1100–2414) constructs from the sequence of mouse tNASP (GenBank™ accession number AF034610) were used for recombinant protein production. Affinity-purified antibodies were prepared as described (31) using immobilized N-terminal recombinant protein.

Western Blots

Proteins were separated on 10–20% gradient minigels (Bio-Rad) and transblotted to Immobilon-P (Waters Inc., Bedford, MA), either stained for protein or blocked, and probed with anti-NASP antiserum as described (32). In blots used to assess the expression of NASP in HeLa and 3T3 cells, the blots were stained with amido black for protein to ensure equal loading, computer-imaged with a desktop scanner, destained, and immunostained with anti-NASP. Protein lysates of mouse embryo, spleen, and testis were made by grinding the minced tissue in a Dounce homogenizer with PBS and Protease Inhibitor Mixture Set 1 (Calbiochem) at the recommended dilution. The suspension was frozen, thawed, and centrifuged at 12,000 × *g*. After centrifugation, the supernatant was extracted (twice in chloroform and methanol (3:1)) and the volatile solvents removed by vacuum centrifugation (10 min). Protein concentrations were determined using Micro BCA protein detection reagents (Pierce).

Immunohistochemistry

Mouse tissue sections and embryos were fixed in Bouin's solution, paraffin-embedded, sectioned, and incubated with rabbit anti-recombinant N-terminal NASP (affinity-purified) as primary antiserum. This antiserum recognizes both somatic and testicular NASP protein. Immunostaining was carried out as described (33).

Indirect Immunofluorescence

Cell cultures were grown on microscope slides with wells (Lab-Tek II chamber slides, Nalgene-Nunc, Naperville, IL). Medium was removed by aspiration and the cells washed twice with cold (4 °C) PBS. Methanol (−20 °C) was added to fix the cells (10 min, −20 °C). The cells were washed twice with cold PBS, blocked in 2% normal goat serum (20 min), and washed with cold PBS (twice, 5 min each). Rabbit anti-NASP or preimmune serum was added to each well (1:500 in PBS and 0.1% bovine serum albumin), the cells were incubated (45 min) and washed in PBS (3 times, 5 min each), and fluorescein isothiocyanate-labeled goat anti-rabbit antiserum was added (1:1000 in PBS and 0.1% bovine serum albumin) for a 30-min incubation followed by three washes in PBS. The cells were also stained with propidium iodide (0.01 mg/ml, 10 min) and washed (3 times in PBS) before the plastic wells were removed.

Cell Culture

66-2 mouse myeloma cells (34) were maintained in Dulbecco's modified Eagle's medium-H plus 10% horse serum at 37 °C and 5% CO_2. HeLa cells, mouse 3T3 fibroblasts, and CV-1 cells were maintained in Dulbecco's modified Eagle's medium-H plus 10% calf serum.

Cell Cycle Studies

Thymidine Block—To obtain populations of cells in G_2-phase, HeLa cells were arrested by double-thymidine block. Cells were blocked for 18 h with 2 mM thymidine, released for 9 h by washing out the thymidine, and blocked again with 2 mM thymidine for 17 h to arrest all of the cells at the beginning of S-phase. The cells were released by washing out the thymidine and total RNA and lysates prepared from samples taken at specific time points after release from thymidine.

Serum Starvation—At 72 h after plating 3T3 cells, complete medium was removed, cells were washed three times with medium alone and incubated with Dulbecco's modified Eagle's medium containing 0.5% calf serum for 48 h. At time 0 h, the low serum medium was removed, and the cells were stimulated by addition of medium containing 10% serum.

The cell cycle positions of the HeLa and 3T3 cells were determined by analyzing the DNA content of propidium iodide-stained cells from each time point at the UNC Flow Cytometry Facility. Total cell RNA was prepared for the cell cycle studies using the Ultraspec RNA isolation system (Biotecx Laboratories Inc., Houston, TX). Cell lysates were prepared by washing the collected cells in PBS followed by lysis in 1% SDS and boiling for 5 min. In all cell cycle studies, equal RNA loading was verified by probing Northern blots with G3PDH, and the position of the cells in the cell cycle was monitored using FACS analysis (shown for Fig. 6).

Affinity Purification

Rabbit antibodies to recombinant mouse NASP were affixed to Reactigel 6X (Pierce) and were used to affinity purify native NASP and its associated histones from lysates. Myeloma 66-2 cell pellets were thawed on ice and resuspended in phosphate-buffered saline (PBS) with the addition of Protease Inhibitor Mixture I and Proteasome Inhibitor I (Calbiochem). Cell debris was pelleted in a microcentrifuge at maximum speed, and the supernatant was mixed with the NASP:Reactigel beads and rocked overnight at 4 °C. A column was made from the beads and was washed extensively with several volumes of PBS before elution with Immunopure elution buffer (Pierce). Collected fractions were immediately neutralized with 1 M Tris-Cl, pH 8.5, and elution of protein was tracked at 280 nm. Pooled fractions were dialyzed in 10,000 molecular weight cutoff Slidealyzer cassettes (Pierce) *versus* several changes of 1/20× PBS and lyophilized.

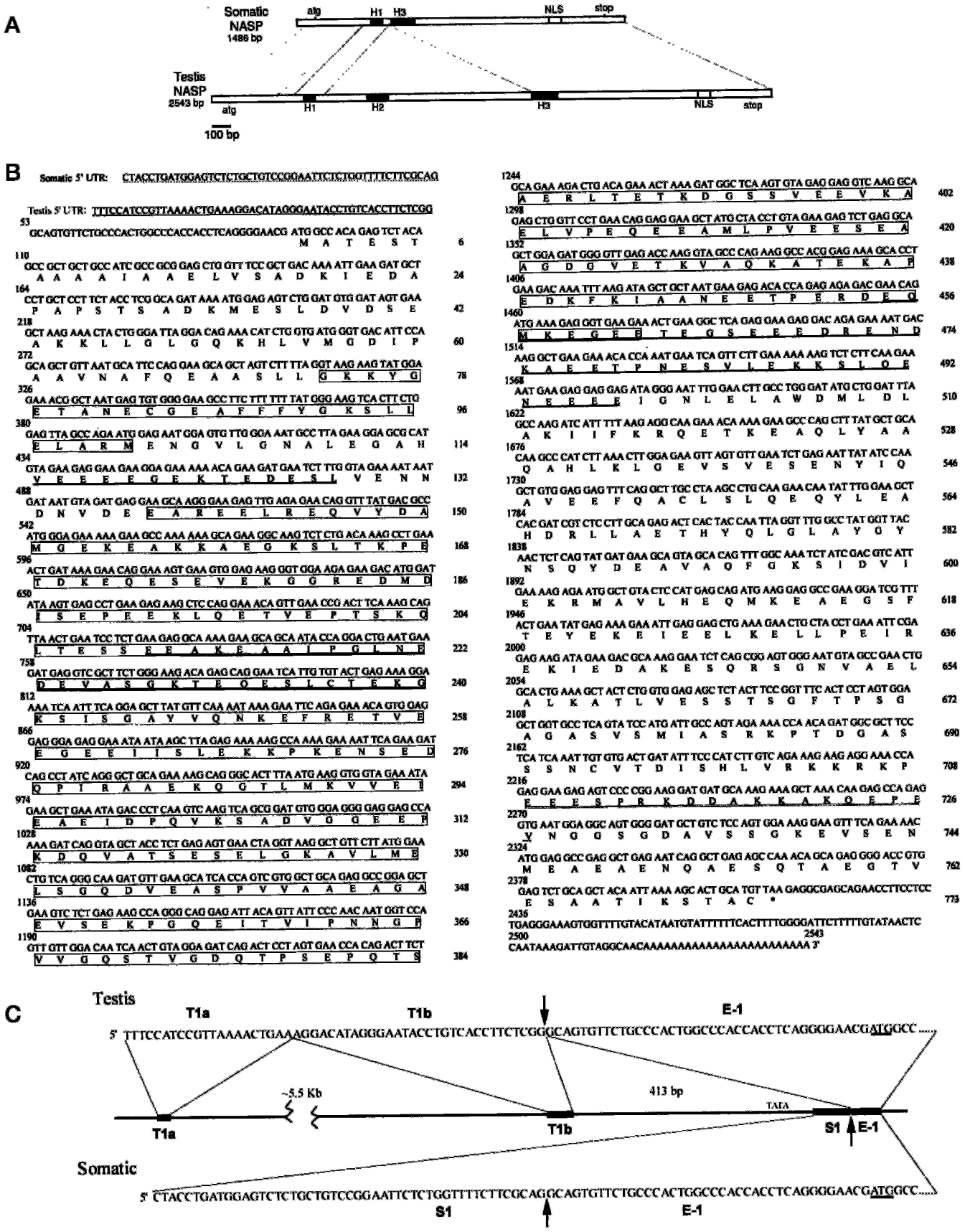

FIG. 1. **Comparison of somatic and testicular NASP.** *A*, somatic and testicular NASP. The open reading frames are identical except for the deletion of two separate regions, reducing the size of tNASP from 773 to 421 amino acids in sNASP. *H1, H2*, and *H3*, histone binding domains. *NLS*, nuclear localization signal. *B,* the cDNA sequence for mouse tNASP is 2543 bp with a start codon at nucleotides 92–94 and a TAA stop codon at nucleotides 2411–2413, encoding a protein of 773 amino acids (M_r 83,934). The cDNA sequence for somatic NASP is generated by substituting the *dashed underlined* 5′UTR sequence (*somatic 5′UTR*) for the *single underlined* portion of the sequence (*testis 5′ UTR*) and by deleting the two regions of the sequence that are *boxed*. The sNASP cDNA contains the same start and stop codons as tNASP and encodes a 421-amino acid protein

Isolation of Histones

H1 proteins from mouse myeloma cells or affinity-purified NASP were isolated as described by Brown and Sittman (35). Core histones were isolated from the perchloric acid-insoluble pellet by extraction with 0.2 M H_2SO_4, precipitated with trichloroacetic acid or 8 volumes of cold acetone, and washed with acetone, 0.01 M HCl. All procedures were done at 4 °C. Mouse histone H1 cDNAs (kindly provided by Dr. D. Sittman, University of Mississippi Medical Center) were expressed from a pET-11d vector. The histone H1 constructs were transformed into the BL21 (DE3) bacterial host cell line and the recombinant proteins purified using the T7 tag affinity purification kit (Novagen, Madison, WI) according to the manufacturer's instructions.

Reverse-phase HPLC

Lyophilized histones were dissolved in 0.1% trifluoroacetic acid and applied to a C-18 reverse-phase column (Waters, DeltaPak, 15 μM, 300 Å, 3.9 × 300 mm) equilibrated with acetonitrile and 0.1% trifluoroacetic acid. Proteins were eluted at 28 °C with a multistep acetonitrile in 0.1% trifluoroacetic acid gradient (0.7 ml/min). Gradients were developed from 18.5 to 100% buffer B (90% acetonitrile in 0.1% trifluoroacetic acid) and 81.5 to 0% buffer A (10% acetonitrile in 0.1% trifluoroacetic acid). Protein elution was monitored at 220 nm. Fractions were collected, dried by vacuum centrifugation, and analyzed by SDS-polyacrylamide gel electrophoresis.

Histone Labeling

Biotin labeling of histones was performed as described (4). The binding of labeled histones to streptavidin-agarose was used to test the efficiency of biotinylation, and bound and unbound fractions were analyzed by SDS-polyacrylamide gel electrophoresis.

Co-immunoprecipitation

For binding experiments, rNASP (2 μg) was mixed with biotin-labeled histone H1 recombinants in a 500-μl volume of 0.5× Tris-buffered EDTA and incubated for 1 h at room temperature with gentle shaking. Precipitation was carried out with either streptavidin or affinity-purified anti-rNASP antibodies. The samples were loaded on 10–20% SDS-polyacrylamide gels.

RESULTS

Sequences of Somatic and Testicular Mouse NASP—In the course of our studies on tNASP, it was of interest to ask whether or not the fertilizing spermatozoon would carry NASP into the unfertilized egg (5). However, contrary to expectations (2), NASP was detected with an anti-NASP antibody in the germinal vesicle of growing oocytes within the ovary (see Fig. 9*E*). Subsequent screening of an ovarian cDNA library resulted in the isolation of a cDNA encoding sNASP, which differed from tNASP, suggesting that the ovarian cDNA was an alternatively spliced transcript. As a result of this observation, we began an extensive search for the presence of NASP in embryonic and somatic tissues. Fig. 1*A* shows the relationship between sNASP and tNASP cDNAs. The sNASP is identical to tNASP except for the deletion of the two separate regions, shown in Fig. 1*A*, reducing the size of sNASP to 421 amino acids (45,752 Da) from the 773 amino acids of tNASP (83,934 Da). The sequence for mouse tNASP (Fig. 1*B*), obtained by screening a mouse testis cDNA library, yielded a 2543-bp consensus sequence. The sequence for sNASP (Fig. 1*B*), obtained from the mouse ovary cDNA library yielded a consensus sequence of 1486 bp, which differs from tNASP cDNA in the 5′ UTR as well as in the deletion of two portions of the coding region. To confirm the sequence of sNASP in other somatic tissues, the complete sNASP coding region from spleen cDNA, generated by PCR, was sequenced and found to be identical to ovary sNASP (data not shown). The lack of two tNASP regions in the sNASP mRNA and the presence of differing sequences in the upstream portion of the 5′ UTR of sNASP are most likely explained by differential pre-mRNA splicing events and different promoters. Fig. 1*C* shows the relevant 5′ UTR sequences for the two NASP forms, indicating how the 5′ ends of the transcripts are alternatively spliced from the genomic sequence. The 5′ end of the testis mRNA arises by the splicing of two small exons (*T1a* and *T1b*, Fig. 1*C*) onto the 5′ end of exon one (*E-1*). The unique portion of the 5′ UTR of sNASP, (*S1*, Fig. 1*C*) is contiguous with the sequence (*E-1*) common to both sNASP and tNASP. A 3′ splice is evident at the end of S1 (Fig. 1*C*). The splice junctions of the exons have been identified by sequencing genomic DNA (not shown).

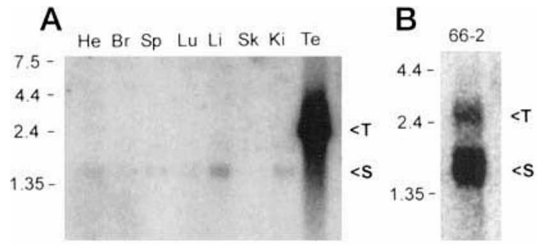

FIG. 2. **Northern blot analysis of NASP expression The blots were probed with a ^{32}P-labeled cDNA representing full-length tNASP.** <*T*, tNASP, <*S*, sNASP. *A,* 2 μg of poly(A)$^+$ RNA from heart (*He*), brain (*Br*), spleen (*Sp*), lung (*Lu*), liver (*Li*), skeletal muscle (*Sk*), kidney (*Ki*), and testis (*Te*). *B,* 2 μg of poly(A)$^+$ RNA from 66-2 mouse myeloma cells.

The deduced mouse tNASP protein sequence is 81% identical to human tNASP and retains the three histone binding sites (Fig. 1*A*) previously identified in human tNASP (4). Additionally, the sNASP-deduced protein sequence has the same structural features found in all tNASP sequences (36), including a nuclear localization signal, a leucine zipper, and an ATP/GTP binding site.

Northern Blot Analysis—Probing a multiple tissue Northern blot (CLONTECH) of mouse tissues with the tNASP coding region cDNA revealed a strong signal in mouse testis at 2.7 kb (<T) and a weaker signal at 1.7 kb (<S) in mouse liver, kidney, spleen, brain, and heart (Fig. 2*A*). Probing 66-2 mouse myeloma cell RNA revealed a strong 1.7-kb (<S) signal and a weaker 2.7-kb (<T) signal (Fig. 2*B*). To assay a wider variety of tissues for NASP expression, a mouse mRNA master blot was probed with the tNASP coding region. As shown in Fig. 3*A*, testis mRNA showed the strongest signal, at least five times that found in 11-day-old embryos. Densitometeric analysis of the blot without the testis signal (Fig. 3*B*) revealed that the other most predominant signals were found in the thymus, spleen, ovary, and all embryonic stages, with peak expression on day 11. Epididymal tissue expressed approximately 20% of the 11-day-old embryo level, whereas all other tissues, including mRNAs from mouse brain, eye, liver, lung, kidney, heart, skeletal muscle, smooth muscle, pancreas, thyroid, submaxillary gland, prostate, and uterus, had weak signals (<20%).

PCR Analysis of NASP Transcript Tissue Distribution—PCRs were performed with primers specific for the coding region common to both mouse sNASP and tNASP, employing a multiple tissue cDNA panel as the source of cDNA templates, including cDNAs from heart, brain, spleen, lung, liver, skeletal muscle, kidney, testis, and 7-, 11-, 15-, and 17-day embryos (Fig. 4). Agarose gel analysis of the PCR products showed the

(M_r 45,751). The histone binding domains are *single underlined*, and the nuclear translocation signal is *double-underlined*. Nucleotide *numbers* refer to the tNASP sequence. The GenBank™ accession numbers are AF034610 (tNASP) and AF095722 (sNASP). *C,* genomic structure of NASP encoding the alternately spliced 5′ UTRs of somatic and testis NASP. The genomic sequence is diagrammed as the *thin centerline* with exons shown as wider bands. In tNASP, the 5′ UTR includes *T1a* and *T1b* spliced onto the 5′ end of exon one (*E-1*). In sNASP, the 5′ UTR includes *E-1* and an additional 49 bp, *S1*, not present in tNASP. A TATA box for the somatic form is indicated ~30 bp upstream of the transcription initiation site.

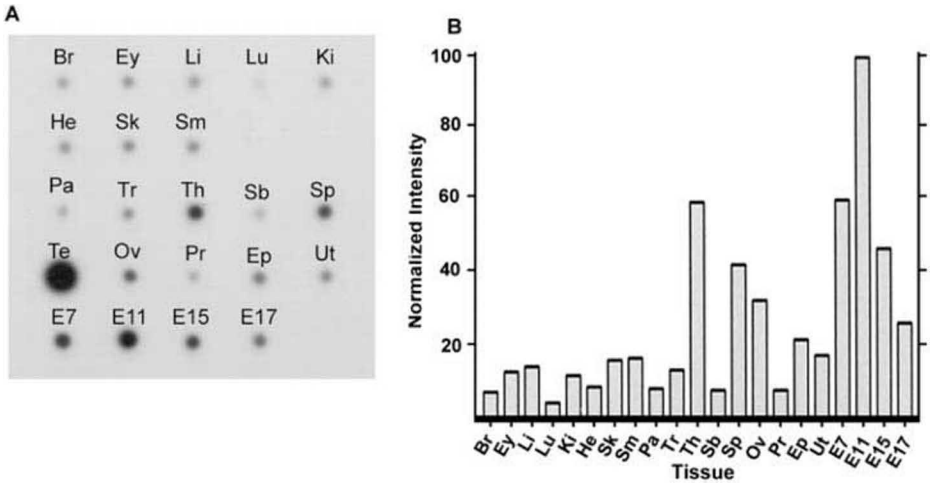

FIG. 3. **Dot blot analysis of NASP expression.** *A*, RNA master blot (CLONTECH) representing 18 different mouse tissues and 4 stages of embryonic development normalized to 8 different housekeeping genes probed with a ^{32}P-labeled cDNA representing full-length tNASP. The tissues included are brain (*Br*), eye (*Ey*), liver (*Li*), lung (*Lu*), kidney (*Ki*), heart (*He*), skeletal muscle (*Sk*), smooth muscle (*Sm*), pancreas (*Pa*), thyroid (*Tr*), thymus (*Th*), submaxillary gland (*Sb*), spleen (*Sp*), testis (*Te*), ovary (*Ov*), prostate (*Pr*), epididymis (*Ep*), uterus (*Ut*), and embryonic stages 7, 11, 15, and 17 (*E7, E11, E15, E17*). *B,* relative image intensities were quantified using Gel Expert software. The intensities are normalized to the day 11 embryo signal. The testis signal (not shown on graph) was more than five times greater than the E11 signal.

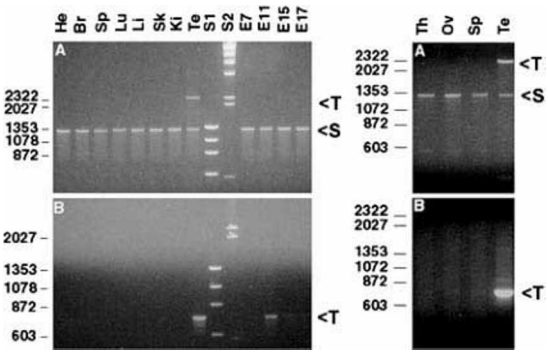

FIG. 4. **Mouse multiple tissue cDNA panel.** Testis and somatic NASP were detected by PCR. cDNAs included are from the heart (*He*), brain (*Br*), spleen (*Sp*), lung (*Lu*), liver (*Li*), skeletal muscle (*Sk*), kidney (*Ki*), and testis (*Te*), as well as embryonic (*E*) stages from day 7, 11, 15, and 17. Additional cDNAs were prepared using thymus (*Th*) and ovary (*Ov*), but these were not normalized to the expression of housekeeping genes. In both *A panels*, primers specific to the common coding regions of testicular (2319 bp) and somatic (1363 bp) NASP were used. In both *B panels*, primers specific to a 725-bp sequence of tNASP were used. Standards were: S1, ϕX174, *Hae*III digest; and S2, λgt11, *Hin*dIII digest. <*T*, tNASP, <*S*, sNASP.

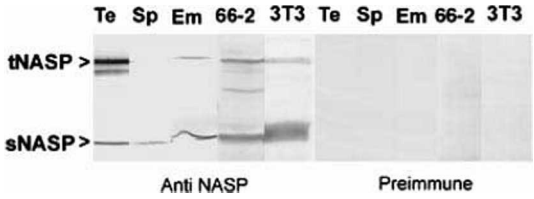

FIG. 5. **Western blot analysis of NASP protein expression.** Lysates were prepared from mouse testis (*Te*), spleen (*Sp*), day 11 embryos (*Em*), 66-2 mouse myeloma cells, and mouse NIH-3T3 cells (*3T3*). 20 μg of each lysate were run on a 10–20% gradient SDS-polyacrylamide gel electrophoresis, blotted, and probed with either anti-recombinant NASP or preimmune serum. The *arrowheads* indicate sNASP at 62 kDa and tNASP at 138 kDa.

presence of a 2319-bp tNASP band only in the testis (<T, Fig. 4*A*). However, all tissues, including the testis, produced a 1263-bp sNASP band (<S, Fig. 4*A*). The PCRs of testis RNA were clearly inefficient in this assay, as the Northern blots show very little sNASP compared with tNASP in the testis (Fig. 2*A*), probably because of the large size of the amplified testis fragments. Therefore, PCRs were performed using the cDNA panel and primers specific for a 725-bp sequence specific to tNASP from nucleotides 334 to 1059. Agarose gel analysis of these products showed 725-bp bands only from the testis and embryos, with a strong signal on day 11 but with faint signals in the other embryonic stages (<T, Fig. 4*B*). Embryonic stage cDNAs did not give a 2319-bp band when amplified with common tNASP and sNASP coding region primers because of the inefficient amplification of the tNASP cDNA.

Western Blot Analysis of Native NASP—Western blots of lysates (equal protein loading) from mouse testis, spleen, embryos, mouse 66-2 myeloma cell line, and mouse 3T3 cells were probed with anti-NASP antibodies. A strong tNASP band of 138 kDa was present in the testis, in myeloma cells, and in 3T3 cells, with a somewhat weaker band in embryos (Fig. 5). An sNASP band of 62 kDa was present in all of the lysates (Fig. 5). These results support the data presented in Figs. 2–4, which show that tNASP is present in 3T3 cells, myeloma cells, and embryos but not in the spleen (Figs. 2–4). Only sNASP is present in spleen.

The addition of protease inhibitors to the lysates did not prevent the appearance of immunoreactive NASP breakdown products, particularly in the myeloma extract. No significant bands were seen when blots were probed with preimmune serum (Fig. 5). Recombinant 6-His-tagged tNASP also migrated at 138 kDa (data not shown). The anomalous migration of NASP and other similar nuclear proteins after SDS-polyacrylamide gel electrophoresis has been observed and discussed previously (1).

NASP mRNA Regulation during the Cell Cycle—The level of NASP mRNA was assayed in an asynchronous, exponentially growing population of HeLa cells and in double thymidine-blocked cells allowed to progress in synchrony through the cell cycle. In double thymidine-locked cells at the G_1/S border (t = 0, Fig. 6*A*), there was little, if any, sNASP and relatively little tNASP mRNA present. However, as cells were released from the G_1/S block and entered S-phase, increased levels of NASP mRNA were detected (t = 2, 4, and 6 h, Fig. 6, *A* and *C*). Asynchronously dividing cells expressed an intermediate level of NASP mRNA (*AS*, Fig. 6*A*). As expected, histone H4 mRNA levels were low at the G_1/S border in blocked cells and increased significantly as cells progressed through S-phase (Fig. 6*A*), particularly relative to the G3PDH controls.

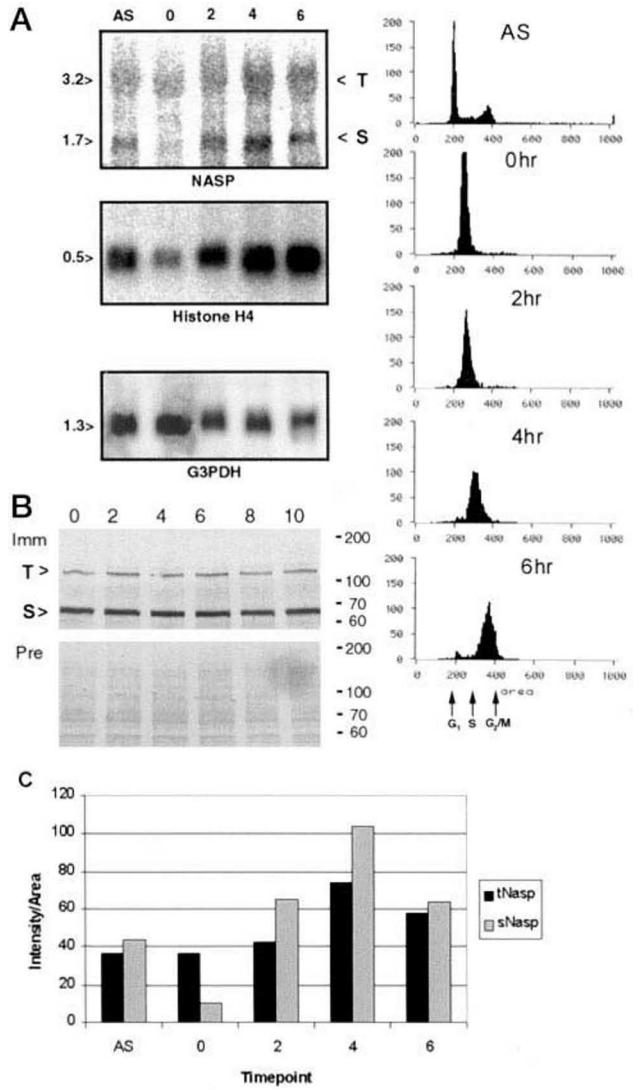

FIG. 6. **Cell cycle regulation of NASP expression in HeLa cells.** *A*, Northern blots of RNA isolated from an asynchronous, exponentially growing population of HeLa cells and from double thymidine-blocked cells allowed to progress in synchrony through the cell cycle, probed with full-length tNASP. *AS*, asynchronously dividing HeLa cells. $t = 0$, G_1/S border; $t = 2$, 4, and 6 h as the cells progressed through S-phase. The *right panel* shows the FACS analysis demonstrating the progression of the cells through the cell cycle for the time points assayed. <*T*, tNASP, <*S*, sNASP. *B,* Western blot analysis of NASP present in parallel cultures of synchronous HeLa cell lysates up to 10 h following release from the thymidine block. *Imm*, anti-NASP; *Pre*, preimmune serum. *T*>, indicates tNASP at 138 kDa, and *S*> indicates sNASP at 62 kDa. *C,* bar graph representing the relative intensities of the tNASP (<*T*) and sNASP (<*S*) bands shown in *A*.

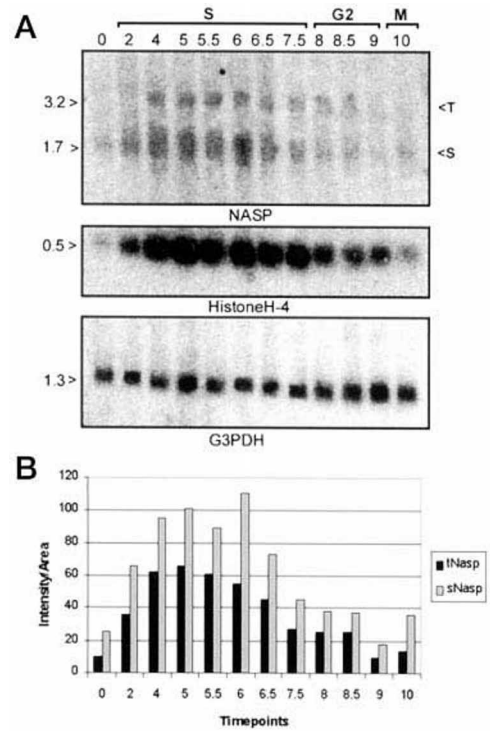

FIG. 7. **Cell cycle regulation of NASP mRNA in HeLa cells.** *A*, Northern blots of RNA isolated from double thymidine-blocked cells allowed to progress in synchrony through the cell cycle, probed with full-length tNASP. As in Fig. 6*A*, $t = 0$, G_1/S border. NASP mRNA was assayed over a 10-h period. *S*, S-phase, G_2, G_2-phase, *M*, mitosis, <*T*, tNASP, <*S*, sNASP. *B,* bar graph representing the relative intensities of the tNASP (<*T*) and sNASP (<*S*) bands shown in *A*.

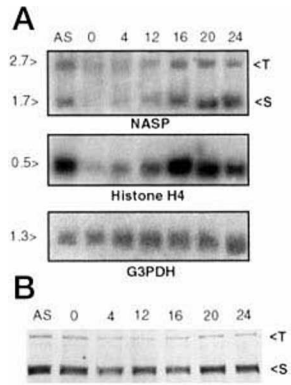

FIG. 8. **Cell cycle regulation of NASP expression in mouse 3T3 fibroblasts.** *A*, the level of NASP mRNA was assayed by probing Northern blots with full-length tNASP from asynchronously growing mouse 3T3 fibroblasts (*AS*) from a population of cells that were synchronized by serum starvation. In serum-starved cells ($t = 0$), very low levels of NASP expression were detected. After serum replacement, cells entered S-phase and showed a peak of NASP mRNA by $t = 16$ h. <*T*, tNASP, <*S*, sNASP. *B*, Western blot analysis of NASP expression in parallel cultures of synchronized 3T3 cells. <*T* indicates tNASP at 138 kDa, and <*S* indicates sNASP at 62 kDa.

In a second experiment, time points were taken from G_1/S through mitosis. After 6–6.5 h, NASP mRNA levels began to decrease and were almost undetectable by 10 h, late G_2/M-phase (Fig. 7, *A* and *B*). Similarly, histone H4 mRNA levels began to decrease and were relatively low by 10 h (Fig. 7). In Western blots of lysates from parallel cultures of synchronous HeLa cells, NASP levels remained constant throughout the cell cycle. After release from the thymidine block, protein levels of sNASP and tNASP were not significantly different from those at $t = 0$ (*S*>, *T*>, Fig. 6*B*), consistent with NASP being a relatively stable protein.

NASP and histone H4 mRNA levels were also assayed in 3T3 cells. In cells starved for serum for 48 h ($t = 0$), very low levels of NASP mRNA were detected (Fig. 8). After serum replenishment, some cells entered S-phase at about 12 h, and the majority entered by 16 h, when there were significantly increased levels of both NASP and histone H4 mRNA by 16 h (Fig. 8). Western blots of 3T3 cells growing in culture demonstrated that NASP levels remained constant throughout the cell cycle (Fig. 8*B*) in the same manner as observed in HeLa cells (Fig. 6*B*). However, CV-1 cells that had been confluent for 8 days and were not dividing showed little or no NASP present, indicating the eventual loss of NASP protein in nondividing cells (Fig. 10*E*, see below). To ensure the balanced loading of RNA in each well of each gel shown in Figs. 6–8, all blots were also probed

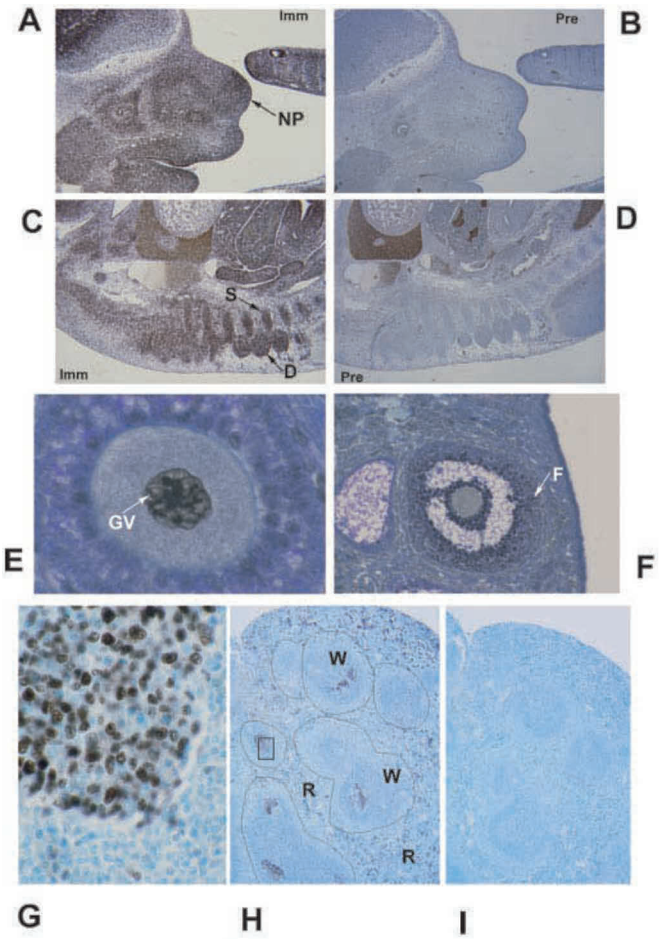

FIG. 9. **Immunohistochemical localization of NASP.** Mouse tissues were probed with affinity purified rabbit anti-recombinant NASP antibodies (*A, C, E, F, G*, and *H*) or preimmune rabbit IgG (*B, D*, and *I*). Sections were counter-stained with toluidine blue. *A–D*, 11.5 day mouse embryo. *A* and *C*, nuclear staining is evident throughout the embryo, particularly in areas of dense cell proliferation, including the nasal process (*NP*) and brain, and in the somites (*S*) and dorsal (*D*) root ganglia. *Imm*, anti-NASP; *Pre*, preimmune serum. *B* and *D*, control sections show peroxidase-positive blood cells (*D*) but no specific staining for NASP. *E* and *F*, ovary. *E*, NASP is present in the germinal vesicle (nucleus, *GV*) of an oocyte in a secondary follicle. *F*, during the rapid proliferation of granulosa cells in growing follicles (*F*), NASP is evident in the nuclei of the corona radiata cells and in granulosa cells lining the antrum. No staining was seen in control sections. *G–I*, spleen. *H*, NASP is present in clustered groups of cells within germinal centers of the white pulp (*W*) and in cells scattered throughout the splenic cords of the red pulp (*R*). Areas of white pulp (*W*) are *outlined*. The *box* indicates an area of *H* seen at higher magnification in *G*. *I*, no staining was seen in control sections. *G*, NASP nuclear localization is clearly evident in the nuclei of proliferating lymphocytes.

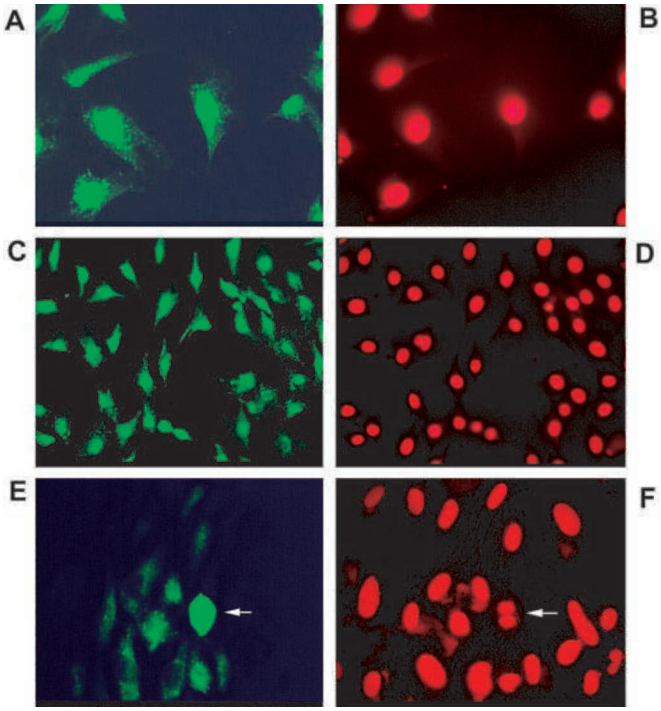

FIG. 10. **Immunofluorescent localization of NASP in mouse 3T3 fibroblasts and CV-1 cells.** Mouse 3T3 fibroblasts were cultured to 50% confluence (*A–D*), and CV-1 cells were maintained as a confluent, contact-inhibited culture for 8 days (*E* and *F*). The cells were stained with either propidium iodide (*B, D*, and *F*) or rabbit anti-recombinant NASP antibodies followed by a fluorescein isothiocyanate-labeled goat anti-rabbit IgG (*A, C*, and *E*). 3T3 cells show mainly nuclear staining (*A* and *C*). All cells in the culture contain NASP (*A–D*). In contrast, after 8 days, most CV-1 cells showed little or no NASP (*E* and *F*), except when cells were in the mitotic cycle (*arrow, E* and *F*).

for the housekeeping gene *G3PDH*. Similar *G3PDH* bands at all times sampled indicated an equal loading of RNA at each time period.

Localization of NASP—Fig. 9 demonstrates the localization of NASP in embryonic and somatic tissues. In the 11.5-day mouse embryo (Fig. 9, *A–D*) most cells in the embryo are positive for NASP. Nuclear staining was particularly evident throughout areas of dense cell proliferation as seen in the nasal process (*NP*) and brain (Fig. 9*A*) and in the cervical somites (*S*) and dorsal (*D*) root ganglia (Fig. 9*C*). Control sections stained with preimmune serum showed peroxidase-positive blood cells but no specific staining for NASP (Fig. 9, *B* and *D*).

In the ovary, sNASP is present in the germinal vesicle ((*GV*) nucleus) of primary oocytes in both primary and secondary follicles (Fig. 9*E*). Occasional staining was seen in oocytes within primordial follicles. During the rapid proliferation of granulosa cells in the growing follicle (*F*), NASP is evident in those cells adjacent to the zona pellucida (corona radiata) and those lining the developing antra (Fig. 9*F*).

In the spleen, sNASP is present in clustered groups of cells within germinal centers of the white pulp (*W*, Fig. 9*H*). The nuclear localization of NASP is clearly evident in these proliferating lymphocytes (Fig. 9*G*). NASP is also seen in cells scattered throughout the splenic cords of the red pulp (*R*, Fig. 9*H*). Control sections showed no staining (Fig. 9*I*).

In 3T3 cells growing in culture, NASP was primarily localized in the nucleus (Fig. 10, *A–D*). In these cultures, which were approximately 50% confluent, every cell contained NASP (compare Fig. 10, *A* and *B*, *C* and *D*). In contrast, cultures of CV-1 cells that had been confluent for 8 days had very few mitotic cells (compare Fig. 10, *E* and *F*) and showed little or no NASP present in either the cytoplasm or nucleus (Fig. 10*E*) of most cells. This finding is consistent with the loss of NASP mRNA as cells exit S-phase and slow degradation of the NASP protein in the arrested cells (Fig. 7). However, the occasional CV-1 cell that entered mitosis in these cultures showed strong staining for NASP (*arrow*, Fig. 10*E*), indicating a strong correlation between the presence of NASP and the growth state of the cells.

Histone Interaction with NASP—To characterize the functional role of NASP as a histone-binding protein in somatic cells, the histones bound to native NASP in myeloma 66-2 cells were characterized. Native NASP was isolated from the soluble fraction of mouse myeloma cells by affinity-purified anti-recombinant NASP antibody column chromatography (data not shown). Histones were extracted from the isolated native NASP complex and the histone types present in the affinity-purified NASP complex identified by reverse-phase HPLC.

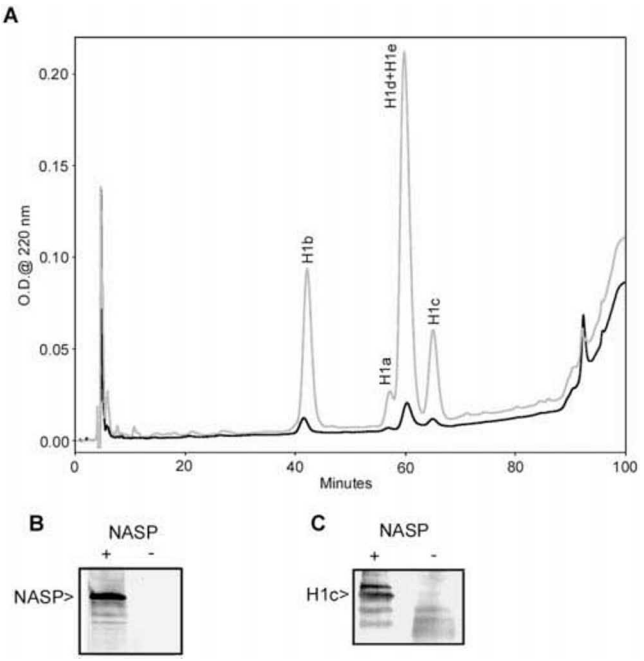

FIG. 11. **H1 linker histones and mouse myeloma NASP.** *A*, reverse-phase HPLC separation and identification of mouse histones bound to affinity-purified native NASP. Total mouse myeloma H1 variants (*gray trace*) and NASP bound H1 variants (*black trace*). *B*, precipitation of complexes of biotin-labeled recombinant histone H1c and recombinant NASP with streptavidin followed by Western blotting with anti-rNASP antibodies. *C*, immunoprecipitation of biotin-labeled recombinant histone H1c and rNASP. Pre-assembled complexes (+ or − *NASP*) were immunoprecipitated with anti-rNASP antibodies. Western blotting was performed using alkaline phosphatase-conjugated avidin. Histone H1c was detected in the antibody-precipitated fraction.

Based on our standard elution profiles of purified mouse myeloma cell core and linker histones, only the linker histones (variants *H1a, H1b, H1c*, and *H1d/e*) were found to co-purify with native NASP (Fig. 11*A*). No core histones were present in the sulfuric acid extracts. To confirm the binding of H1 subtypes, they were expressed in *Escherichia coli* as recombinants, purified, labeled with biotin, and used to reconstitute the complex with recombinant NASP. Fig. 11*B* shows that NASP was detected in the streptavidin-precipitated fraction when biotin-labeled recombinant H1c and recombinant NASP were incubated together. Conversely, by immunoprecipitation of the complexes with anti-NASP antibodies, the histone H1c protein was associated with the immunoprecipitated fraction (Fig. 11*C*).

DISCUSSION

In this study, we have demonstrated that the histone-binding protein NASP is present in dividing somatic cells and coupled to the cell cycle. Importantly, it appears that in myeloma cells NASP is complexed only with H1 linker histones and that the complex can be reconstructed *in vitro* with recombinant NASP and histones, implying that NASP functions to transport and/or store H1 histones in this cell line. sNASP is a shortened version of the testicular form of NASP, lacking two separate regions of the tNASP protein sequence (Fig. 1). This is a result of alternative splicing of the NASP pre-mRNA, skipping exons 4 and 6 (data not shown). Significantly, sNASP retains its characteristic features, namely two of the three histone binding sites, a nuclear localization signal, a leucine zipper, and an ATP/GTP binding site (36). We have further demonstrated the presence of NASP mRNA and protein in a variety of mouse somatic tissues, including mouse embryonic cells (Figs. 2–5, 9, and 10). Moreover, NASP mRNA accumulation is cell cycle-dependent, increasing during S-phase, concomitant with increased histone mRNA accumulation, and declining in G_2, even in continually cycling cells (Figs. 6–8). Consequently, since we have previously demonstrated that NASP functions as a histone-binding protein with a nuclear localization signal (4), our present data suggest that sNASP plays an important role during the cell division cycle, providing for the more rapid and efficient transport of histones into the nucleus. Additionally, NASP might also provide for non-chromatin-bound storage of linker histones.

Additional support for the presence of somatic NASP was found from searches of GenBank™ (37), where EST sequences have been reported from various developmental stages, skin, melanoma, neuroepithelium, and mammary gland. Somatic NASP-like sequences also appear in the human EST data base, and in GenBank™ there is a partial sequence for an "autosomal cDNA variant of human testis nuclear autoantigenic sperm protein from primary human peripheral blood mononuclear cells" (GenBank™ accession number AF035191), which has the same overall structure as mouse sNASP. tNASP EST sequences have been reported from the testis, embryo, and transformed cells.

The coupling of NASP mRNA accumulation to the cell cycle (Figs. 6–8) and the nuclear localization of NASP in dividing 3T3 cells (Fig. 10) in large lymphocytes (lymphoblasts) in the spleen (Fig. 9*G*) and in cells in growing embryonic tissues (Fig. 9, *A* and *C*) imply that NASP has a role in the cell's normal progression through its division cycle. This is also evident from our observation that nonmitotic CV-1 cells and nonmitotic cells in various tissues throughout the body do not have detectable quantities of NASP. Even though NASP protein levels remained constant in cultured cells when they were arrested for only 1 day, they ultimately did lose their NASP (Fig. 10, *E* and *F*). Hence, NASP remains present in cycling cells for some period of time after cells leave the cycle, but eventually (8 days in the case of CV-1 cells) NASP is no longer detectable.

Although the DNA replication-coupled synthesis of histones has been known for many years, early workers recognized that histone gene expression could occur without DNA replication (38). Synthesis of mouse oocyte histone H4 occurs independently of DNA replication during oogenesis (12), and synthesis of testis-specific histones continues during spermatogenesis, long after DNA synthesis for meiosis has finished (4, 39, 40). A number of histone H1 proteins are also synthesized independently of DNA replication (11), and H1 mRNAs, particularly H1c and H1e mRNA, are present in nondividing cells (41). The decoupling of DNA and histone synthesis in certain specific cases such as spermatogenesis and oogenesis would seem to support the need for non-chromatin histone storage proteins. The accumulation of NASP is uncoupled from DNA replication during oogenesis (Fig. 9) and spermatogenesis (5), tissues in which histone mRNA and protein synthesis are also uncoupled from DNA replication. In somatic cells, NASP mRNA appears to follow the histone pattern in that it is coupled to DNA replication. Histone mRNA is regulated transcriptionally and post-transcriptionally (41–43), and NASP mRNA may also be similarly regulated. Indeed, it is quite possible that common regulatory elements exist to ensure the concomitant appearance and disappearance of both histone and NASP mRNAs as well as the persistence of both NASP and histones when they are needed in nondividing cells.

Acknowledgments—We thank Gail Grossman and the Immunohistochemistry Core Facility of the Laboratories for Reproductive Biology for their help and expertise.

REFERENCES

1. Welch, J. E., and O'Rand, M. G. (1990) *Biol. Reprod.* **43,** 569–578
2. Welch, J. E., Zimmerman, L., Joseph, D., and O'Rand, M. G. (1990) *Biol. Reprod.* **43,** 559–568
3. Richardson, R. T., Widgren, E. E., and O'Rand, M. G. (1993) in *Reproductive Immunology* (Dondero, E., and Johnson, P. M., eds) pp. 41–46, Raven Press, New York
4. Batova, I. A., and O'Rand, M. G. (1996) *Biol. Reprod.* **54,** 1238–1244
5. O'Rand, M. G., Richardson, R. T., Zimmerman, L. J., and Widgren, E. (1992) *Dev. Biol.* **154,** 37–44
6. Krohne, G. (1985) *Exp. Cell Res.* **158,** 205–222
7. Kleinschmidt, J. A., Dingwall, C., Maier, G., and Franke, W. W. (1986) *EMBO J.* **5,** 3547–3552
8. Kleinschmidt, J. A., Fortkamp, E., Krohne, G., Zentgraf, H., and Franke, W. W. (1985) *J. Biol. Chem.* **260,** 1166–1176
9. Kleinschmidt, J. A., and Seiter, A. (1988) *EMBO J.* **7,** 1605–1614
10. Dabauvalle, M. C., and Franke, W. W. (1982) *Proc. Natl. Acad. Sci. U. S. A.* **79,** 5302–5306
11. Chiu, I-M., and Marzluff, W. F. (1982) *Biochim. Biophys. Acta* **699,** 173–182
12. Wassarman, P. M., and Mrozak, S. C. (1981) *Dev. Biol.* **84,** 364–371
13. Salik, J., Herlands, L., Hoffmann, H. P., and Poccia, D. (1981) *J. Cell Biol.* **90,** 385–395
14. Ishimi, Y., Kojima, M., Yamada, M., and Hanaoka, F. (1987) *Eur. J. Biochem.* **162,** 19–24
15. Ito, T., Bulger, M., Kobayashi, R., and Kadonaga, J. T. (1996) *Mol. Cell. Biol.* **16,** 3112–3124
16. Watanabe, T. K., Fujiwara, T., Nakamura, Y., Hirai, Y., Mackawa, H., and Takahashi, E. (1996) *Cytogenet. Cell Genet.* **74,** 281–285
17. Rodriguez, P., Munroe, D., Prawitt, D., Chu, L. L., Bric, E., Kim, J., Reid, L. H., Davies, C., Nakagama, H., Loebbert, R., Winterpacht, A., Petruzzi, M. J., Higgins, M. J., Nowak, N., Evans, G., Shows, T., Weissman, B. E., Zabel, B., Housman, D. E., and Pelletier, J. (1997) *Genomics* **44,** 253–265
18. Smith, S., and Stillman, B. (1989) *Cell* **58,** 15–25
19. Smith, S., and Stillman, B. (1991) *EMBO J.* **10,** 971–980
20. Kaufman, P. D., Kobayashi, R., Kessler, N., and Stillman, B. (1995) *Cell* **81,** 1105–1114
21. Verreault, A., Kaufman, P. D., Kobayashi, R., and Stillman, B. (1996) *Cell* **87,** 95–104
22. Lorain, S., Quivy, J-P., Monier-Gavelle, F., Scamps, C., Lecluse, Y., Almouzni, G., and Lipinski, M. (1998) *Mol. Cell. Biol.* **18,** 5546–5556
23. Dilworth, S. M., Black, S. J., and Laskey, R. A. (1987) *Cell* **51,** 1009–1018
24. Almouzni, G., Clark, D. J., Mechali, M., and Wollfe, A. P. (1990) *Nucleic Acids Res.* **18,** 5767–5774
25. Sapp, M., and Worcel, A. (1990) *J. Biol. Chem.* **265,** 9357–9365
26. Kleinschmidt, J. A., Seiter, A., and Zentgraf, H. (1990) *EMBO J.* **9,** 1309–1318
27. Borun, T., Gabrielli, W. F., Asiro, K., Zwiedler, A., and Baglioni C. (1975) *Cell* **4,** 59–67
28. Harris, M. E., Bohni, R., Schneiderman, M. H., Ramamuithy, L., Schumperli, D., and Marzluff, W. F. (1991) *Mol. Cell. Biol.* **11,** 2416–2424
29. Workman, J. L., and Kingston, R. E. (1998) *Annu. Rev. Biochem.* **67,** 545–579
30. Kong, M., Richardson, R. T., Widgren, E. E., and O'Rand, M. G. (1995) *Biol. Reprod.* **53,** 579–590
31. Richardson, R. T., Yamasaki, N., and O'Rand, M. G. (1994) *Dev. Biol.* **165,** 688–701
32. Richardson, R. T., Nikolajczyk, B. S., Abdullah, L. H., Beavers, J. C., and O'Rand, M. G. (1991) *Biol. Reprod.* **45,** 20–26
33. Sivashanmugam, P., Richardson, R. T., Hall, S., Hamil, K. G., French, F. S., and O'Rand, M. G. (1999) *J. Androl.* **20,** 384–393
34. Laskov, R., and Scharff, M. D. (1970) *J. Exp. Med.* **131,** 515–521
35. Brown, D. T., and Sittman, D. B. (1993) *J. Biol. Chem.* **268,** 713–718
36. O'Rand, M. G., Batova, I., and Richardson, R. T. (2000) in *The Testis* (Goldberg, E., ed) Serono Symposium, pp. 143–150, Springer, New York
37. Altschul, S. F., Gish, W., Miller, W., Meyers, E. W., and Lipman, D. J. (1990) *J. Mol. Biol.* **215,** 403–410
38. Waithe, W. I., Renaud, J., Nadeau, P., and Pallotta, D. (1983) *Biochemistry* **22,** 1778–1783
39. Meistrich, M. L., Bucci, L. R., Trostle-Weige, P. K., and Brock, W. A. (1985) *Dev. Biol.* **112,** 230–240
40. Kim, Y. J., Hwang, I., Tres, L. L., Kierszenbaum, A. L., and Chae, C. B. (1987) *Dev. Biol.* **124,** 23–34
41. Wang, Z-F., Sirotkin, A. M., Buchold, G. M., Skoultchi, A. I., and Marzluff, W. F. (1997) *J. Mol. Biol.* **271,** 124–138
42. Heintz, N., Sive, H. S, and Roeder, R. G. (1983) *Mol. Cell. Biol.* **3,** 539–550
43. Sittman, D. B., Graves, R. S., and Marzluff, W. F. (1983) *Proc. Natl. Acad. Sci.* **80,** 1849–1853